Supporting Information

Bis(cholyl)-based chloride channels with oxalamide and hydrazide selectivity filters

Rashmi Sharma, Amal Vijay, Arnab Mukherjee* and Pinaki Talukdar*

Chemistry Department, Indian Institute of Science Education and Research Pune
Dr. Homi Bhabha Road, Pashan, Pune 411008, Maharashtra (India)
E-mail: arnab.mukherjee@iiserpune.ac.in, ptalukdar@iiserpune.ac.in

Table of Content

I. General Methods:

All chemical reactions were performed under a nitrogen atmosphere. All reagents and solvents for synthesis were purchased from commercial sources (Sigma-Aldrich, Spectrochem) and used further without purification. The column chromatography was carried out using Merc silica (100-200 / 230-400 mesh size). The thin layer chromatography was performed on E. Merck silica gel 60-F254 plates. Egg yolk phosphatidylcholine (EYPC) as a solution of chloroform (25 mg/mL), mini extruder, polycarbonate membrane of 100 nm and 200 nm were purchased from Avanti Polar Lipid. HEPES, HPTS, Lucigenin, NaOH, Triton-X, and all inorganic salts were obtained as molecular biology grade from Sigma-Aldrich.

II. Physical Measurements:

The ^{1}H NMR spectra were recorded at 400 MHz whereas ^{13}C at 101 MHz. The residual solvent signals were considered as an internal reference ($CDCl_3$ δ_H = 7.26 ppm, DMSO–d_6 δ_H = 2.50, CD_3CN δ_H = 1.94) to calibrate spectra. The chemical shifts were reported in ppm. Following abbreviations were used to indicate multiplicity patterns m: multiplet, s: singlet, d: doublet, t: triplet, q: quartet, dd: doublet of doublet, td: triplet of doublet. Coupling constants were measured in Hz. Infra-red (IR) spectra were measured in cm^{-1} using a FT–IR spectrophotometer. Melting points were measured on a micro melting point apparatus. High-resolution mass spectra (HRMS) were recorded on an electrospray ionization time-of-flight (ESI-TOF). Fluorescence experiments were recorded on a Fluoromax-4 from Jobin Yvon Edison equipped with an injector port and magnetic stirrer in a microfluorescence cuvette. All buffer solutions were prepared from the autoclaved water. Adjustment of pH of buffer solutions was made using a Helmer pH meter. The extravesicular dye was removed by performing gel chromatography using Sephadex G-50. The fluorescence data were processed using OriginPro 8.5.

III. Synthesis:

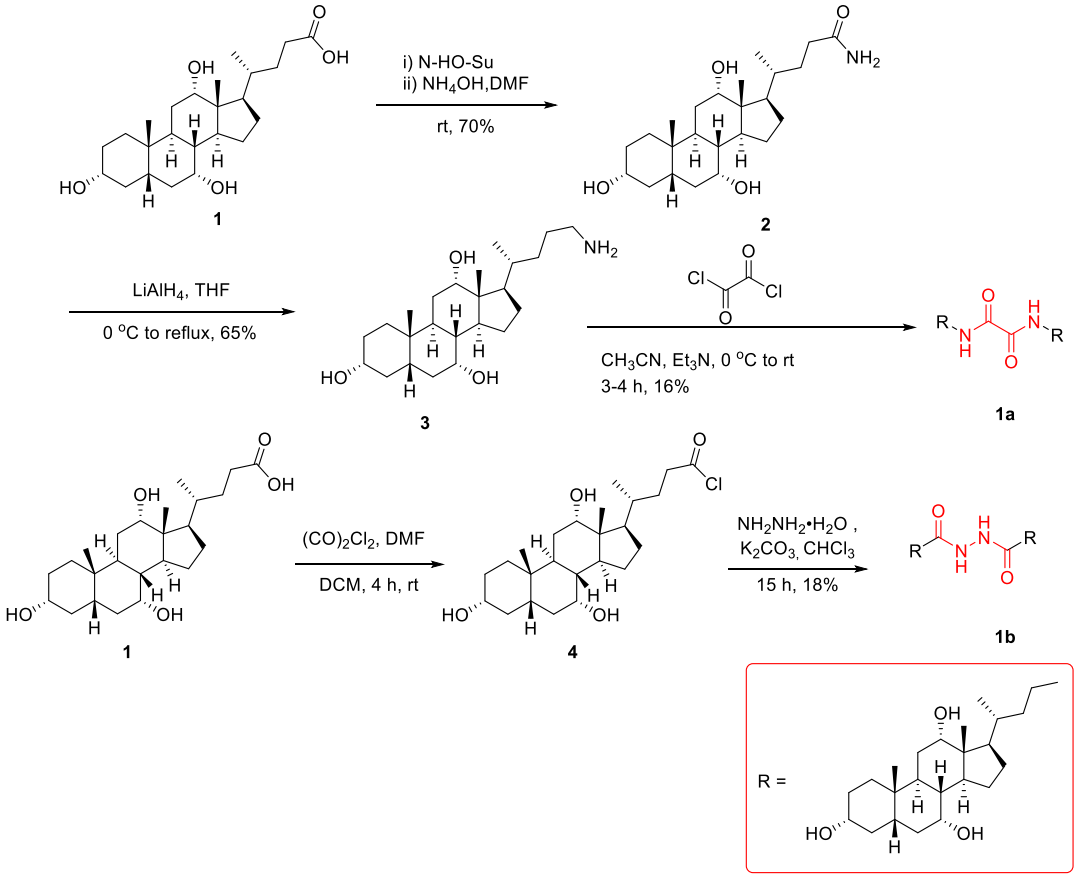

Scheme S1. Synthesis of oxalamide derivative **1a** and hydrazide derivative **1b**.

Synthesis of compound 2: Synthesis of compound **2** was done according to known protocol.[S1] Cholic acid (1.07 g, 2.62 mmol), DCC (590 mg, 2.86 mmol), and *N*-hydroxysuccinimide (430 mg, 3.78 mmol) were dissolved in anhydrous THF and CH_3CN (10:1 mL), and stirred at room temperature for 8 h. After completion of the reaction, the white solid formed was filtered out and the filtrate was concentrated *in vacuo* to give a white foam (88% yield). A portion of this solid (230 mg, 0.70 mmol) was dissolved in anhydrous DMF and NH_4OH (27% aqueous solution) was added. After 12 h of stirring at 50 °C, the mixture was poured into brine. The precipitate was collected by suction filtration, washed with water (2 × 10 mL), and purified with column chromatography over silica gel using CH_2Cl_2/CH_3OH (8:1) as the eluent to give **2** (214 mg, 75% yield) as white powder. ^{1}H NMR spectrum was matched with the data of the reported compound.

Synthesis of compound 3: Synthesis of compound **3** was also done according to known protocol.[S1] Compound **2** (310 mg, 0.76 mmol) was dissolved in anhydrous THF under N_2. $LiAlH_4$ (288 mg, 7.60 mmol) was added slowly. The reaction mixture was heated to reflux for 12 h. A small amount of ethyl acetate was added slowly to quench the $LiAlH_4$, which was then filtered and the filtrate was collected and concentrated *in vacuo*. The residue was purified with column chromatography over silica gel using CH_2Cl_2/CH_3OH (10:1) and CH_3OH/Et_3N (50:1) as the eluents to give **3** (194 mg, 65% yield) as white solid. ^1H NMR spectrum of the synthesized compound was matched with reported data.

Synthesis of compound 1a: Compound **4** (400 mg, 1.01 mmol) was dissolved in anhydrous THF (15 mL) under N_2. Triethylamine (0.63 mL, 0.45 mmol) was added dropwise to a solution of amine at 0 °C. Oxalyl chloride (0.19 mL, 0.22 mmol) was added dropwise and stirred at room temperature for 14 h. The precipitate was filtered off, and the solution was evaporated in vacuo. The pure product **1a** was isolated by flash column chromatography over silica gel using CH_2Cl_2/CH_3OH (10:1) as white solid (185 mg, 16% yield). **M.P.:** 165-167 ºC; **IR** (neat, ν/cm^{-1}): 3418, 2930, 2864, 1713, 1635, 1552, 1461, 1378, 1304, 1167, 977;). **^{1}H NMR (400 MHz, DMSO-*d*$_6$, δ):** 7.96 (d, *J* = 7.5 Hz, 1H), 4.33 (d, *J* = 3.9 Hz, 2H), 4.11 (s, 2H), 4.01 (s, 2H), 3.77 (d, *J* = 7.6 Hz, 2H), 3.60 (s, 2H), 3.42 (s, 2H), 3.17 (s, 2H), 3.06 (s, 2H), 2.89 (s, 2H), 2.73 – 2.59 (m, 2H), 2.15 (ddd, *J* = 23.9, 18.5, 11.8 Hz, 6H), 1.97 (dd, *J* = 19.6, 9.8 Hz, 4H), 1.78 (d, *J* = 12.9 Hz, 4H), 1.64 (d, *J* = 12.7 Hz, 9H), 1.41 (s, 6H), 1.35 (s, 6H), 1.23 (s, 9H), 1.14 – 1.11 (m, 2H), 0.92 (s, 6H), 0.80 (s, 6H), 0.58 (s, 6H). **^{13}C NMR (101 MHz, DMSO-*d*$_6$):** 169.49, 71.32, 70.70, 66.55, 46.28, 45.93, 41.69, 35.48, 35.07, 34.61, 33.62, 32.61, 31.21, 30.52, 29.20, 28.76, 27.59, 26.44, 24.10, 23.04, 22.80, 22.44, 17.45, 14.90, 12.56. **HRMS (ESI):** Calc. for $C_{52}H_{86}N_2O_8$ $[M+H]^+$: 841.6228; Found: 841.6201.

Synthesis of compound 1b: To a solution of Cholic acid (500 mg, 1.22 mmol) and DMF (0.1 mL) in CH_2Cl_2 (60 mL) was added oxalyl chloride (0.51 mL, 0.60 mmol) dropwise at 0 °C. The reaction mixture was then stirred at room temperature for 2 h, and distilled in vacuo to afford cholyl chloride as a colorless liquid (522 mg). Cholyl chloride (209 mg, 0.49 mmol) was added to a solution of hydrazine monohydrate (118 μL, 0.24 mmol) and K_2CO_3 (1.00 g) in $CHCl_3$ (10 mL) at 0 °C. The reaction mixture was stirred at same temperature for 1 h, and then allowed to warm to room temperature. After 18 h, the compound was extracted with ethyl acetate (3 × 50 mL). The organic

layer was dried over Na_2SO_4 and then evaporated in vacuo. The crude product was purified with column chromatography over silica gel using $CHCl_3$/CH_3OH (10:1) as the eluents to give **1b** as white solid (75 mg, 18% yield). **M.P.:** 145-147 °C; **IR** (neat, ν/cm^{-1}): 3435, 2925, 2854, 1744, 1630, 1460, 1381, 1184, 1083, 1031, 909. **^{1}H NMR (400 MHz, DMSO-*d*$_6$, δ):** 11.89 (s, 2H), 4.31 (d, *J* = 4.4 Hz, 2H), 4.11 (d, *J* = 3.5 Hz, 2H), 4.00 (d, *J* = 3.4 Hz, 2H), 3.78 (d, *J* = 2.8 Hz, 2H), 3.61 (s, 2H), 3.43 (d, *J* = 60.9 Hz, 2H), 3.24 – 3.10 (m, 4H), 2.34 – 2.25 (m, 2H), 2.21 (dd, *J* = 10.4, 4.2 Hz, 2H), 2.12 (dd, *J* = 19.0, 6.5 Hz, 4H), 1.99 – 1.94 (m, 2H), 1.79 (dd, *J* = 14.4, 4.8 Hz, 4H), 1.68 – 1.65 (m, 2H), 1.62 (s, 2H), 1.47 – 1.40 (m, 6H), 1.34 (dd, *J* = 9.9, 4.2 Hz, 4H), 1.23 (s, 12H), 0.92 (d, *J* = 6.4 Hz, 6H), 0.87 – 0.83 (m, 4H), 0.81 (s, 6H), 0.58 (s, 6H). **^{13}C NMR (101 MHz, DMSO-*d*$_6$):** δ 175.52, 71.31, 70.71, 66.53, 47.77, 46.38, 45.96, 41.58, 35.40, 35.05, 34.60, 33.53, 32.40, 31.76, 30.53, 28.72, 27.52, 26.41, 25.51, 24.68, 23.04, 22.82, 17.29, 12.58. **HRMS (ESI):** Calc. for $C_{52}H_{86}N_2O_8$ $[M+H]^+$: 813.5915; Found: 813.5993.

IV. Ion Transport Experiments:[S2]

A. Ion transporting activity studies across EYPC–LUVs⊃HPTS:

Preparation of HEPES buffer and stock solutions: The HEPES buffer of pH = 7.0 was prepared by dissolving an appropriate amount of solid HEPES (10 mM) and NaCl (100 mM) in autoclaved water. The pH was adjusted to 7.0 by addition of aliquots from 0.5 M NaOH solution. The stock solution of all carriers was prepared using HPLC grade DMSO.

Preparation of EYPC–LUVs⊃HPTS in NaCl: In 10 mL clean and dry round bottom flask thin transparent film of egg yolk phosphatidylcholine (EYPC) was formed using a 1 mL EYPC lipid (25 mg/mL in $CHCl_3$) by providing continuous rotation and purging nitrogen gas. The transparent thin film was completely dried under high vacuum for 4-5 h. After that, the transparent thin film was hydrated with the addition of 1 mL HEPES buffer (1 mM HPTS, 10 mM HEPES, 100 mM NaCl, pH = 7.0) and the resulting suspension was vortexted at 10 minutes interval during 1 hour. This hydrated suspension was subjected to 15 cycles of freeze and thaw (N_2 gas, 55 °C) followed by extrusion through 100 nm (pore size) polycarbonate membrane for 21 times, to get vesicles of average 100 nm diameter. The unentrapped HPTS dyes were removed by size exclusion chromatography using Sephadex G-50 (Sigma-Aldrich) with eluting of HEPES buffer (10 mM HEPES, 100 mM NaCl, pH = 7.0). Finally, collected vesicles were diluted to 6 mL to get

EYPC–LUVs⊃HPTS. *Final conditions:* ~ 5 mM EYPC inside: 1 mM HPTS, 10 mM HEPES, 100 mM NaCl, pH = 7.0, outside: 10 mM HEPES, 100 mM NaCl, pH = 7.0.

Ion transport activity by HPTS assay: In a clean and dry fluorescence cuvette, 1975 μL of HEPES buffer (10 mM HEPES, 100 mM NaCl, pH = 7.0) and 25 μL of EYPC–LUVs⊃HPTS vesicle was added. The cuvette was placed in slowly stirring condition using a magnetic stirrer equipped in a fluorescence instrument ($t = 0$ s). The time-dependent HPTS emission intensity was monitored at λ_{em} = 510 nm (λ_{ex} = 450 nm) by creating a pH gradient between intravesicular and extravesicular system by adding 0.5 M NaOH (20 μL) at $t = 20$ s, transporter at $t = 20$ s. Then different concentrations of transporter molecules in DMSO were added at t = 100 s. Finally, the vesicle was lysed by adding of 10% Triton X-100 (25 μL) at $t = 300$ s to destroy the pH gradient (Fig. S1). The time-dependent data were normalized to percent change in fluorescence intensity using Eq. S2:

$$I_F = [(I_t - I_0)/ (I_\infty - I_0)] \times 100) \qquad \text{(Eq. S2)}$$

where, I_0 is the initial intensity, I_t is the intensity at time t, and I_∞ is the final intensity after the addition of Triton X-100.

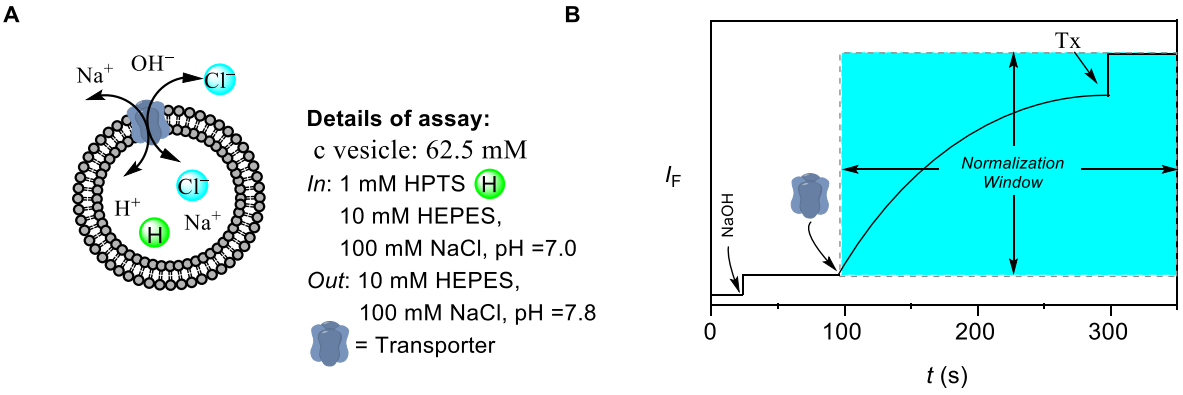

Fig. S1 Representations of fluorescence-based ion transport activity assay using EYPC-LUVs⊃HPTS (A), and illustration of ion transport kinetics showing normalization window (B).

Dose-response activity:

The fluorescence kinetics of each transporter at different concentration was studied as a course of time. The concentration profile data were evaluated at $t = 290$ s to get effective concentration, EC_{50}

(i.e., the concentration of transporter needed to achieve 50 % chloride efflux)[S3] using Hill equation (Eq. S3):

$$Y = Y_\infty + (Y_0 - Y_\infty)/[1 + (c/EC_{50})^n] \qquad \text{(Eq. S3)}$$

where, Y_0 = fluorescence intensity just before the transporter addition (at $t = 0$ s), Y_∞ = fluorescence intensity with excess transporter concentration, c = concentration of transporter compound, and n = Hill coefficient (i.e., indicative for the number of monomers needed to form an active supramolecule).[S4]

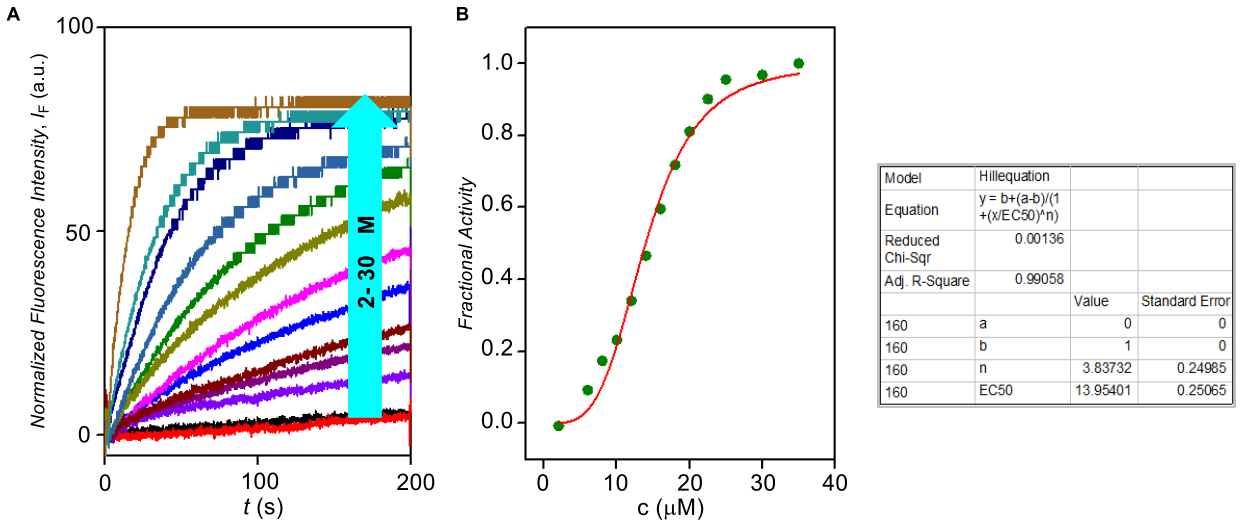

Model	Hillequation		
Equation	y = b+(a-b)/(1 +(x/EC50)^n)		
Reduced Chi-Sqr	0.00136		
Adj. R-Square	0.99058		
		Value	Standard Error
160	a	0	0
160	b	1	0
160	n	3.83732	0.24985
160	EC50	13.95401	0.25065

Fig. S2 Concentration dependent activity of compound **1a** across EYPC–LUVs⊃HPTS (A). Hill plot analysis of compound **1a** (B) at 160 s.

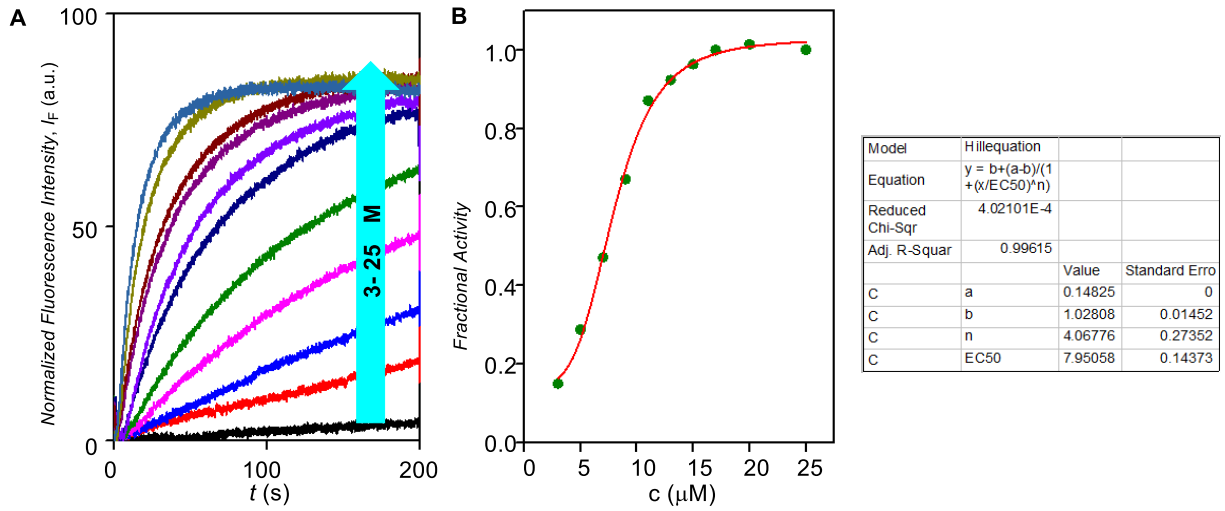

Model	Hillequation		
Equation	y = b+(a-b)/(1+(x/EC50)^n)		
Reduced Chi-Sqr	4.02101E-4		
Adj. R-Squar	0.99615		
		Value	Standard Erro
C	a	0.14825	0
C	b	1.02808	0.01452
C	n	4.06776	0.27352
C	EC50	7.95058	0.14373

Fig. S3 Concentration dependent ion transport activity of compound **1b** across EYPC–LUVs⊃HPTS (A). Hill plot analysis based on the concentration dependent transport activity of compound **1b** (B) at 160 s.

B. Ion selectivity studies across EYPC–LUVs⊃HPTS:

Preparation of EYPC–LUVs⊃HPTS: The vesicles were prepared by the following reported protocol.[S5-S8]

Preparation of buffer and stock solutions: The HEPES buffer solution of 10 mM HEPES and 100 mM salts were prepared by dissolving appropriate amounts of solid HEPES and salts (NaCl, NaF, NaBr, NaI, $NaNO_3$, NaSCN, NaOAc, $NaClO_4$, LiCl, KCl, RbCl, and CsCl) in autoclaved water, followed by adjustment of pH = 7.0 using 0.5 M NaOH. The stock solution of the most active transporter was prepared in HPLC grade DMSO.

Anion selectivity assay: In a clean and dry fluorescence cuvette 1975 μL HEPES buffer (10 mM HEPES, 100 mM NaX, pH = 7.0; where X^- = F^-, Cl^-, Br^-, I^-, OAc^-, NO_3^-, SCN^- and ClO_4^-) was taken, followed by addition of 25 μL EYPC–LUVs⊃HPTS. The resulting solution was slowly stirred in fluorescence instrument equipped with the magnetic stirrer (t = 0 s). The fluorescence intensity of HPTS was observed at λ_{em} = 510 nm (λ_{ex} = 450 nm) as a course of time, with creating pH gradient by addition of 20 μL 0.5 M NaOH at t = 20 s, followed by addition of transporter **1d** (as a DMSO solution) at t = 100 s to initiate ion transport and finally vesicle was lysed for complete destruction of pH gradient by addition of 25 μL 10% Triton X-100 at t = 300 s. The time-dependent

data were normalized to percent change in intensity using Eq. S2 ($I_F = [(I_t - I_0)/(I_\infty - I_0)] \times 100$), where I_0 is the initial intensity, I_t is the intensity at time t, and I_∞ is the final intensity after addition of Triton X-100).

Cation selectivity assay: In a similar way, cation selectivity of transporter **1d** (as a DMSO solution) was explored by changing extravesicular HEPES buffer solution (10 mM HEPES, 100 mM MCl, pH = 7.0) of chloride salts (MCl) of different cations ($M^+ = Li^+, Na^+, K^+, Rb^+, Cs^+$). Using the same condition, no difference in fluorescence intensity was observed for different cations. The fluorescence data were normalised to percent change in intensity as a course of time using Eq. S2 ($I_F = [(I_t - I_0)/(I_\infty - I_0)] \times 100$), where I_0 is the initial intensity, I_t is the intensity at time t, and I_∞ is the final intensity after addition of Triton X-100).

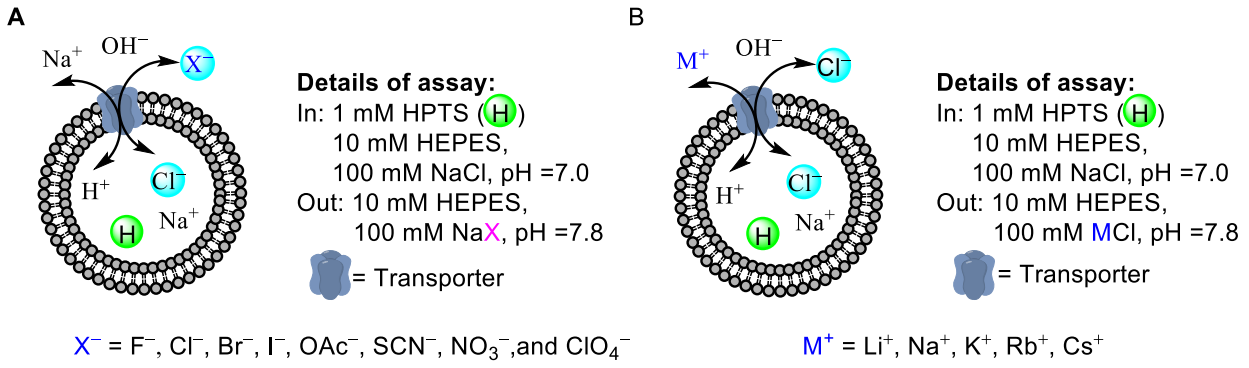

Fig. S4 Schematic representations of fluorescence-based anion (A) and cation selectivity (B) assays.

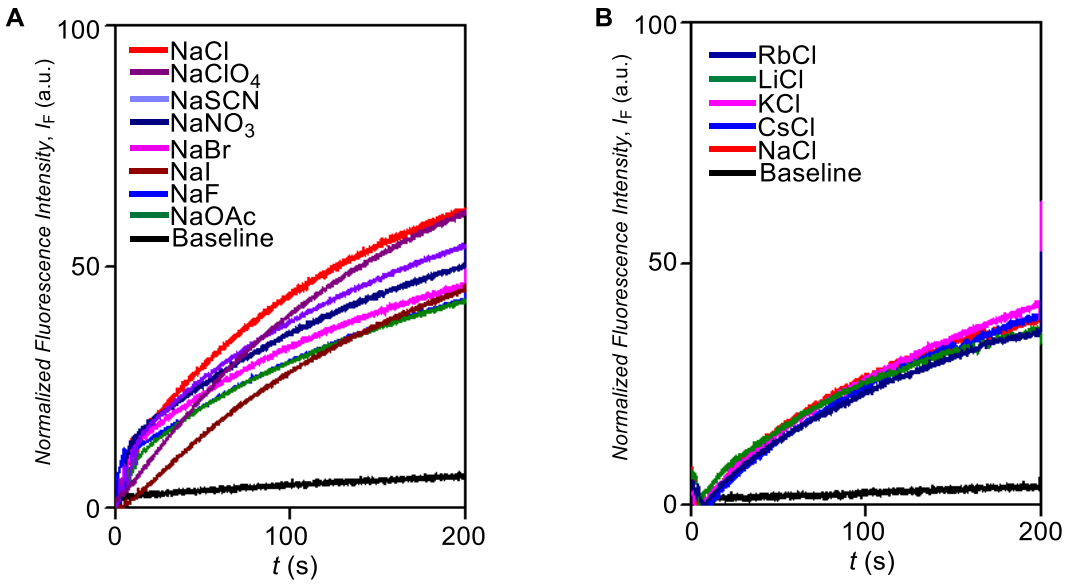

Fig. S5 Anion selectivity of compound **1a** (A) at 17.5 μM and cation selectivity of **1a** (B) at 16.5 μM.

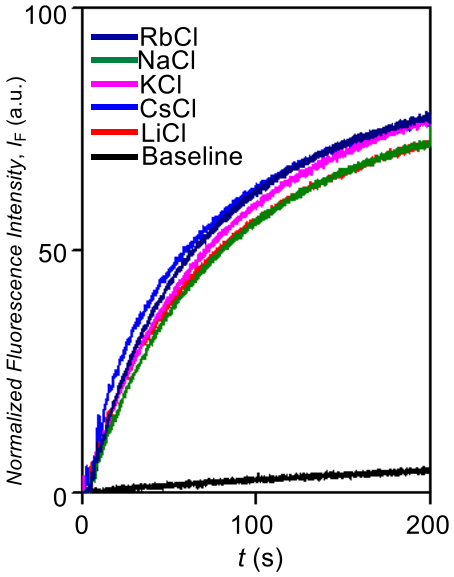

Fig. S6 Cation selectivity of **1b** at 9 μM.

C. Chloride transport activity across EYPC–LUVs⊃lucigenin vesicles:

Preparation of EYPC-LUVs⊃lucigenin vesicles:

In a 10 mL clean and dry round bottom flask the thin transparent film of egg yolk phosphatidylcholine (EYPC) was formed by drying 1 mL egg yolk phosphatidylcholine (EYPC, 25 mg/mL in $CHCl_3$) with providing continuous rotation and purging nitrogen. The transparent thin film was kept on high vacuum for 4 h to remove all trace of $CHCl_3$. Then the transparent thin film was hydrated with 1 mL aqueous $NaNO_3$ (200 mM, 1 mM Lucigenin) with occasional vertexing at 10 minute interval for 1 h. The resulting suspension was subjected for freeze and thaw cycles (≥ 15, liquid nitrogen, 55 °C water bath) and 21 times extrusion through 200 nm pore size polycarbonate membrane. The size exclusion chromatography (using Sephadex G-50) was performed to remove extracellular dye using 200 mM $NaNO_3$ solution as eluent, finally collected vesicles were diluted to 4 mL. Final conditions: ~5 mM EYPC; inside: 200 mM $NaNO_3$, 1 mM lucigenin, pH 7.0; outside: 200 mM $NaNO_3$.

Ion transport activity by Lucigenin assay:

In clean and dry fluorescence cuvette 1975 µL 200 mM $NaNO_3$ solution and 25 µL EYPC-LUVs⊃lucigenin was taken. This suspension was placed in a slowly stirring condition in fluorescence instrument equipped with a magnetic stirrer (at $t = 0$ s). The fluorescence intensity of lucigenin was monitored at $\lambda_{em} = 535$ nm ($\lambda_{ex} = 450$ nm) as a course of time. The chloride gradient was created by addition of 33.3 µL NaCl (2.0 M) at $t = 20$ s between intra and extra vesicular system, followed by addition of transporter at $t = 100$ s. Finally, vesicles were lysed by addition of Triton X-100 at $t = 300$ s for the complete destruction of chloride gradient.

The time-dependent data were normalized to percent change in fluorescence intensity using Eq. S4:

$$I_F = [(I_t - I_0) / (I_\infty - I_0)] \times -100) \qquad \text{(Eq. S4)}$$

where, I_0 is the initial intensity, I_t is the intensity at time t, and I_∞ is the final intensity after the addition of Triton X-100.

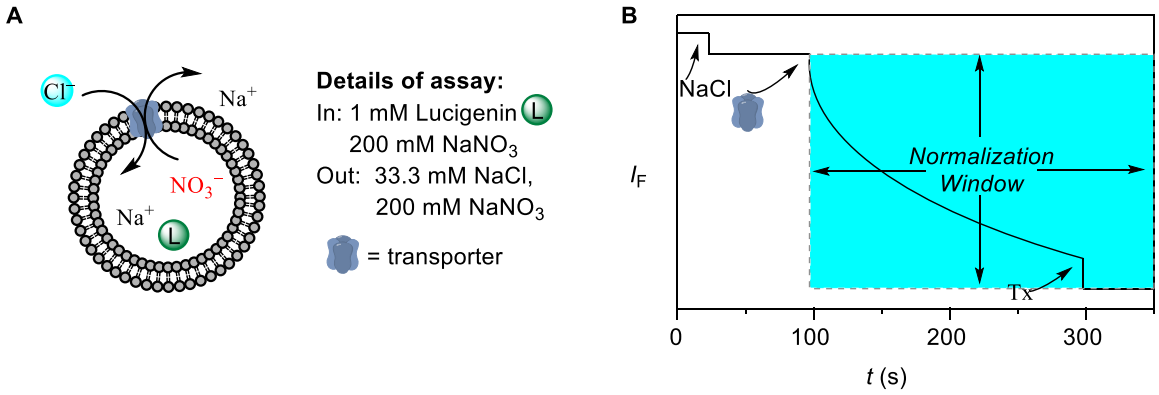

Fig. S7 Representations of fluorescence-based ion transport activity assay using EYPC LUVs⊃lucigenin (A), and illustration of ion transport kinetics showing normalization window (B).

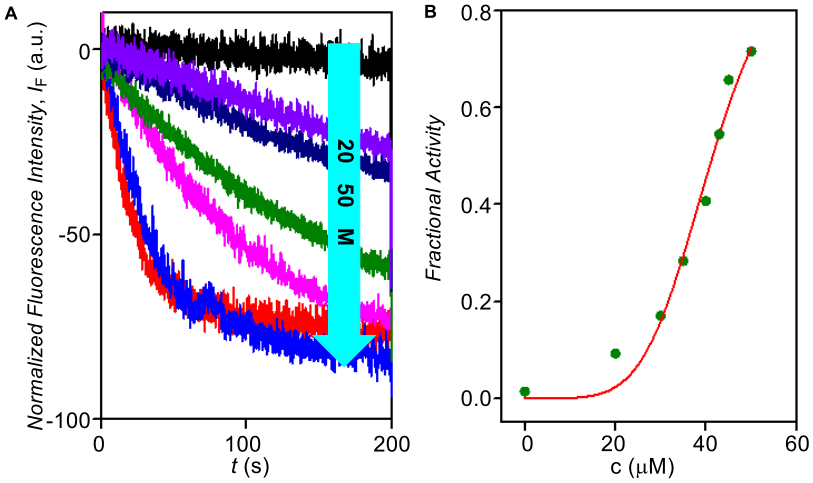

Fig. S8 Concentration dependent activity of compound **1a** across EYPC–LUVs⊃lucigenin. (A). Hill plot analysis of compound **1a** (B).

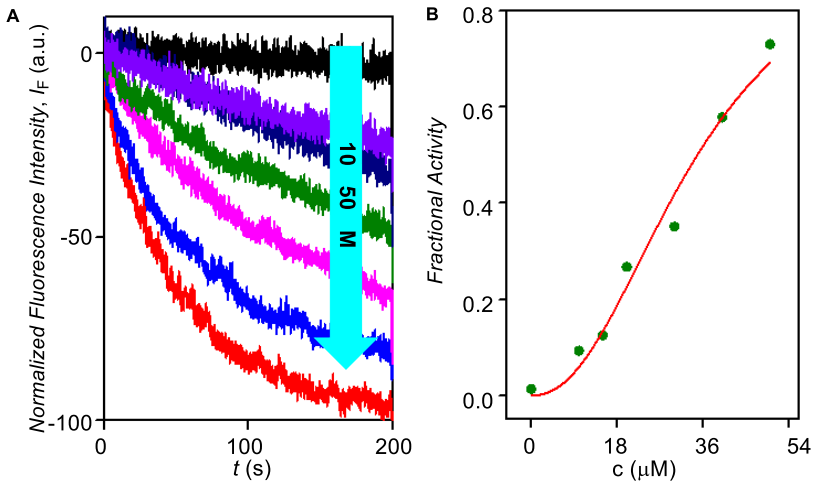

Fig. S9 Concentration dependent activity of compound **1b** across EYPC–LUVs⊃lucigenin (A). Hill plot analysis of compound **1b** (B).

Involvement of cation in transport process:

The involvement of cations in the transport process was evaluated from the lucigenin-based assay. The preparation of solutions and vesicles are similar as described in above section. In assay condition the chloride salt of various cation (M^+ = Li^+, Na^+, K^+, Rb^+ and Cs^+) were added to evaluate the contribution of cation in transport process.

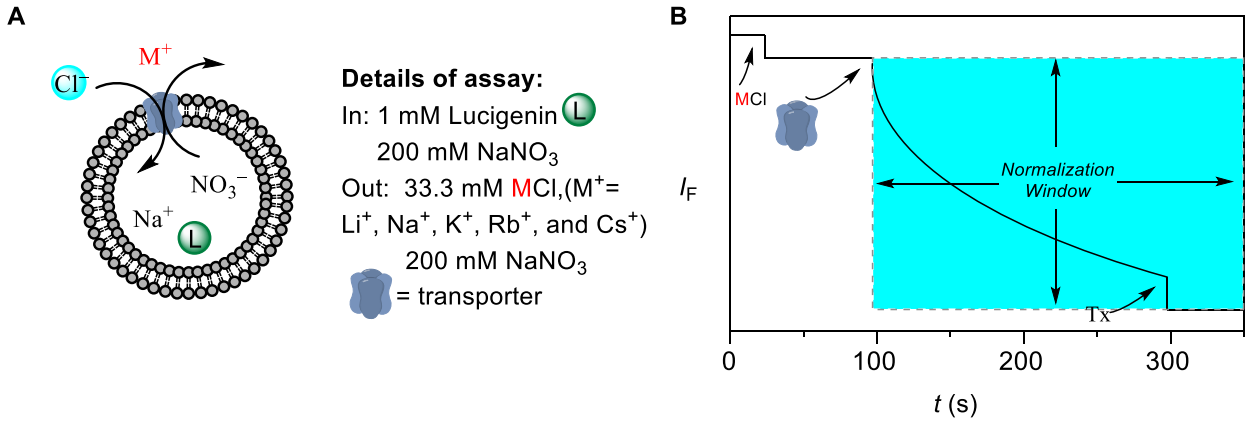

Fig. S10 Representations of chloride influx activity assay using EYPC LUVs⊃lucigenin by varying extravesicular cations (A), and illustration of chloride influx kinetics showing normalization window (B).

Cation transport activity: In a clean and dry fluorescence cuvette 1950 µL of NaNO3 solution (200 mM) was added followed by addition of 50 µL of EYPC/cholesterol- LUVs⊃lucigenin. The cuvette was placed in the fluorescence instrument in slowly stirring condition by a magnetic stirrer equipped with the instrument (at t = 0 s). The time course of lucigenin fluorescence emission intensity, F_t was observed at λ_{em} = 535 nm (λ_{ex} = 450 nm). 33.3 µL of 2 M MCl (M^+ = Li^+, Na^+, K^+, Rb^+ and Cs^+) was added to the cuvette at t = 25 s to create the chloride gradient between the intra and extra vesicular system. Transporter molecules were added at t = 100 s in different concentration and finally 25 µL of 10% Triton X-100 was added at t = 300 s to lyse those vesicles resulting destruction of chloride gradient (Fig. S8).

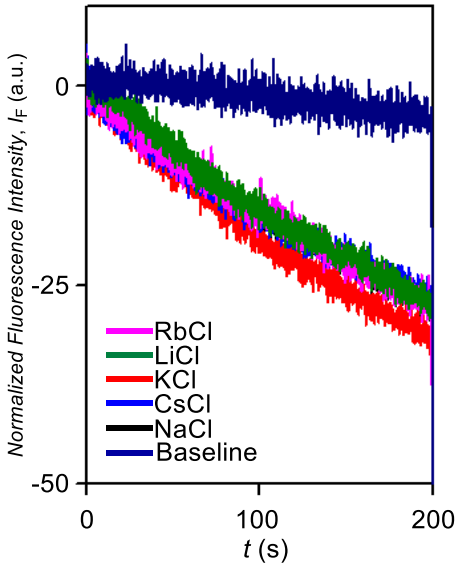

Fig. S11 Influence of extravesicular cations in the Cl^- influx by **1a** at 20 µM.

D. Evaluation of membrane stability and channel nature by ANTS-DPX assay:

EYPC-LUVs were loaded with anionic fluorophore ANTS (8-aminonaphthalene-1,3,6-trisulfonic acid disodium salt) and cationic quencher DPX (1,1-[1,4-phenylenebis(methylene)]bis[pyridinium]bromide) (Fig. S12). Efflux of either ANTS or DPX through pores formed by **1a** was followed by an increase in ANTS emission intensity.

The following buffers were prepared by known method.

Buffer A: 12.5 mM ANTS, 45.0 mM DPX, 5 mM TES, 20 mM KCl, pH = 7.0

Buffer B: 5 mM TES, 100 mM KCl, pH = 7.0.

Preparation of EYPC-LUVs⊃ANTS/DPX vesicles: A thin film of EYPC lipid was prepared by evaporating a solution (1 mL) of EYPC lipid (25 mg/mL) in $CHCl_3$ evaporated slowly by a stream of nitrogen and then in vacuo (6 h), and then hydrated with 1 mL buffer A, followed by vortex treatment (4 times). The resulting suspension was subjected to > 5 freeze-thaw cycles (using liquid N_2 to freeze and a warm water bath to thaw), and 19 times extruded using a Mini-Extruder through a 100 nm polycarbonate membrane (Avanti). External ANTS/DPX was removed by gel filtration (Sephadex G-50) using buffer B and diluted with the same buffer to 3 mL to give EYPC-LUVs⊃ ANTS/DPX stock solution.

ANTS/DPX-assay: In a clean and dry fluorescence cuvette, 50 µL of above lipid solution and 1950 µL buffer B were added. The compound 1a was added at 50 seconds and kept in slowly stirring condition by a magnetic stirrer equipped with the fluorescence instrument (at t = 0 s). The time course of fluorescence emission intensity, F_t was monitored at λ_{em} = 520 nm (λ_{ex} = 353 nm). Finally, at t = 300 s, 25 µL of 10% Triton X-100 was added to lyse all vesicles for 100% dye efflux. Fluorescence intensities (F_t) were normalized to fractional emission intensity I_F using Eq. S4.

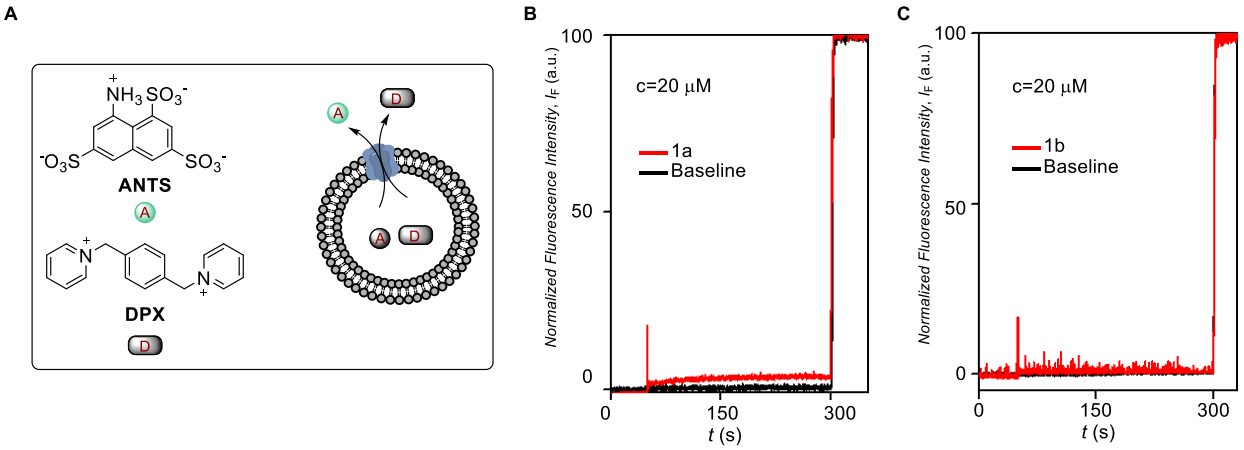

Fig. S12 Representation of ANTS–DPX assay (A) and ANTS–DPX leakage assay in the presence of compound **1a** (B) and compound **1b** (C).

V. Planar Bilayer Conductance Measurements:[S8]

Bilayer membrane (BLM) was formed across an aperture of 150 µM diameter in a polystyrene cup (Warner Instrument, USA) with lipid diphytanoylphosphatidylcholine (Avanti Polar Lipids), dissolved in *n*-decane (18 mg/mL). Both chambers (*cis* and *trans*) were filled with symmetrical solution, containing 1 M KCl. The *trans* compartment was held at virtual ground and the *cis*

chamber was connected to the BC 535 head-stage (Warner Instrument, USA) via matched Ag-AgCl electrodes. Compound **1a** (20 μM) was added to the *trans* chamber and the solution was stirred with a magnetic stirrer for 30 min. Channel formation was confirmed by the distinctive channel opening and closing events after applying voltages. Currents were low pass filtered at 1 kHz using pClamp9 software (Molecular Probes, USA) and an analog-to-digital converter (Digidata 1440, Molecular Probes). All data were analyzed by the software pClamp 9.

The complete data trace observed for ten minutes contained a series of opening and closing events at some indefinite intervals. From a large and complete trace a small portion is presented in the manuscript (Fig. 4A, B). The average current was calculated from this trace and then conductance and other calculations were made accordingly.

Calculation of ion channel diameter: Diameter of artificial ion channel was calculated according to Hille's equation,

$$1/g = (l + \pi d/4) \times (4\rho / \pi d^2) \qquad \text{(Eq. S5)}$$

where, g = corrected conductance (obtained by multiplying measured conductance with the Sansom's correction factor) = 3.37×10^{-10} S, l = length of the ion channel = 34 Å, and ρ = resistivity of the 1 M KCl solution = 9.47 Ω·cm).

Anion selectivity by Planar Bilayer Conductance Measurements:

The *cis* and *trans* chambers were filled with unsymmetric solutions of KCl. The *cis* chamber was filled with 2 M KCl solution and the *trans* chamber was filled with 1 M KCl. The compound **1a** (20 μM) was added to the *trans* chamber and stirred for 20 minutes. The reversal potential was calculated to be 14 ± 2 mV.

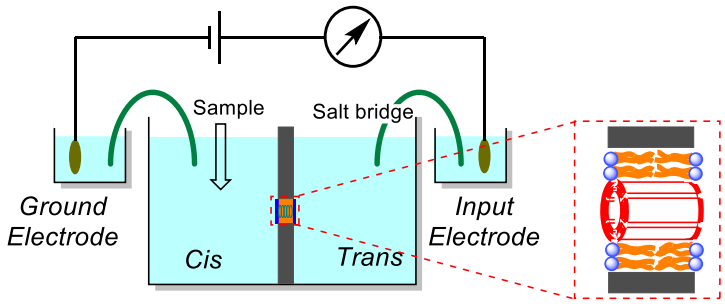

Fig. S13 Systematic representation of black lipid membrane experiment.

VI. Theoretical Studies:

The theoretical calculations were carried out using GROMACS 2019.6 software to get more insights about the pattern of intermolecular hydrogen bonding among the bis(cholyl) derivative units. This optimized hydrazide and oxalamide based channels were then placed in the DPhPC lipid bilayer membrane and constructed two different systems. Afterward, the Molecular Dynamics Simulations were carried out by using an explicit pre-equilibrated phospholipid bilayer of 128 DPHPC (1,2-diphytanoyl-*sn*-glycero-3-phosphocholine) obtained from Lipidbook[S9]. The optimized channel was inserted in a box of 128 POPC molecules using inflategro methodology[S10] at the proper density (area per lipid) of ~ 0.83 nm^2. To solvate the system, ~11000 SPC[S11] model water molecules were added to the system. GROMOS-53a6 united atom force field[S12] was used for DPhPC molecules. The automated topology builder[S13] created by Malde, et al. was used to create the all-atom topology parameters of the channel with GROMOS-53a6[S14] force field. Initially the ions were kept near the bottom of the channel and the system was energy minimized using steepest descent method for 50000 steps. This was followed by equilibration for 1 ns at constant 323 K temperature and 1 bar pressure using Nosé-Hoover thermostat[S15] and Parrinello-Rahman barostat[S16] with a coupling constant of 0.5 ps and 5 ps, respectively. The time step of each simulation was taken as 2 fs. PME[S17] electrostatics was used for electrostatic interactions using a 12 Å cut-off with the van der Waals (vdW) cut-off set at 12 Å. Position restraints of 500 kJ/mol nm^2 is applied to the heavy atoms of the channel molecules. The simulation box was found to be approximately 7.4X7.7X9.0 nm^3 for both the channels. A final 10 ns molecular dynamics simulation at constant 323 K temperature and 1 bar pressure was carried out using Nosé-Hoover thermostat[S15] and Parrinello-Rahman barostat[S16] with a coupling constant of 0.5 ps and 2 ps respectively with similar electrostatics and vdW as in equilibration process. Initially the chloride

ion was placed at the starting of the channels made of hydrazide and oxalamide units. The centre of mass (COM) distance between the channel and the chloride ion was calculated for the 10 ns trajectory (Fig. S14). It was found that the ions get separated from the channel and come to the bulk water within 500 ps in the case of oxalamide channel. While in the case of hydrazide channel it is found that the ions are stabilized at the middle of the channel (COM distance nearly 0 Å) indicating that the individual hydrazide units are stabilizing the chloride ion compared to oxalamide channel. Further, the average interaction energy between the channel molecules was calculated. It is found that the channel – channel interaction is more favored by the oxalamide derivative than that by hydrazide derivative in this case.

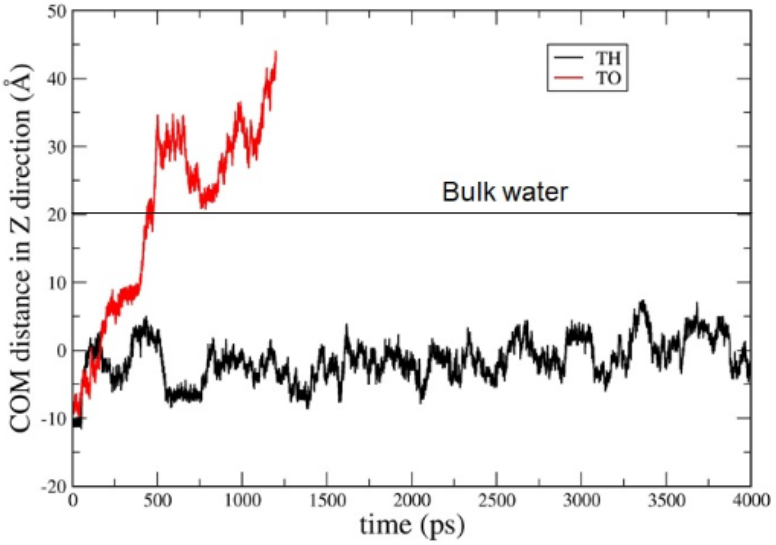

Fig. S14 The centre of mass (COM) distance between the channel and the chloride ion.

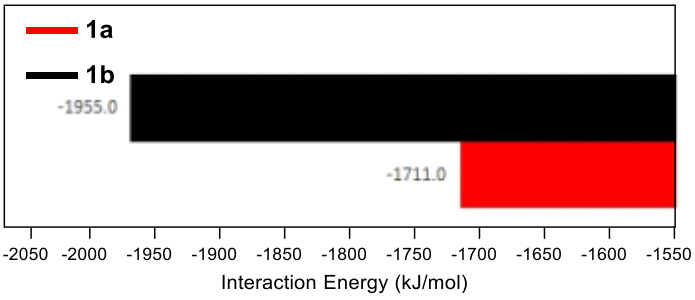

Fig. S15 Bar chart comparing the interaction energy between channels and channel strands.

VII. NMR Spectra:

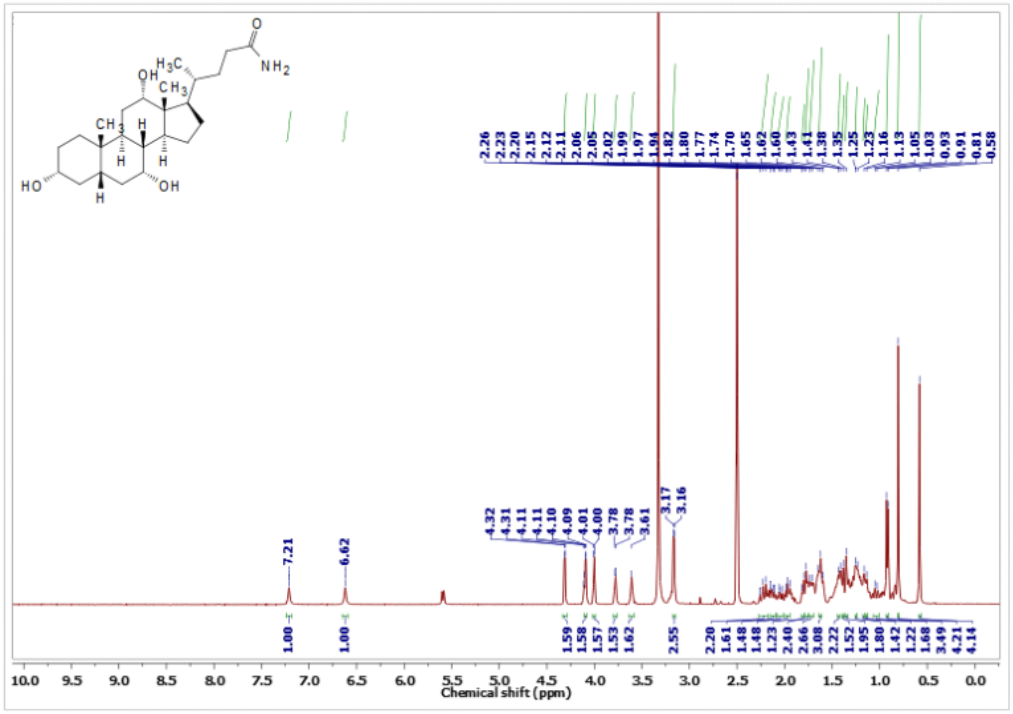

Fig. S16 400 MHz ^{1}H NMR spectrum of **2** in DMSO-d_6.

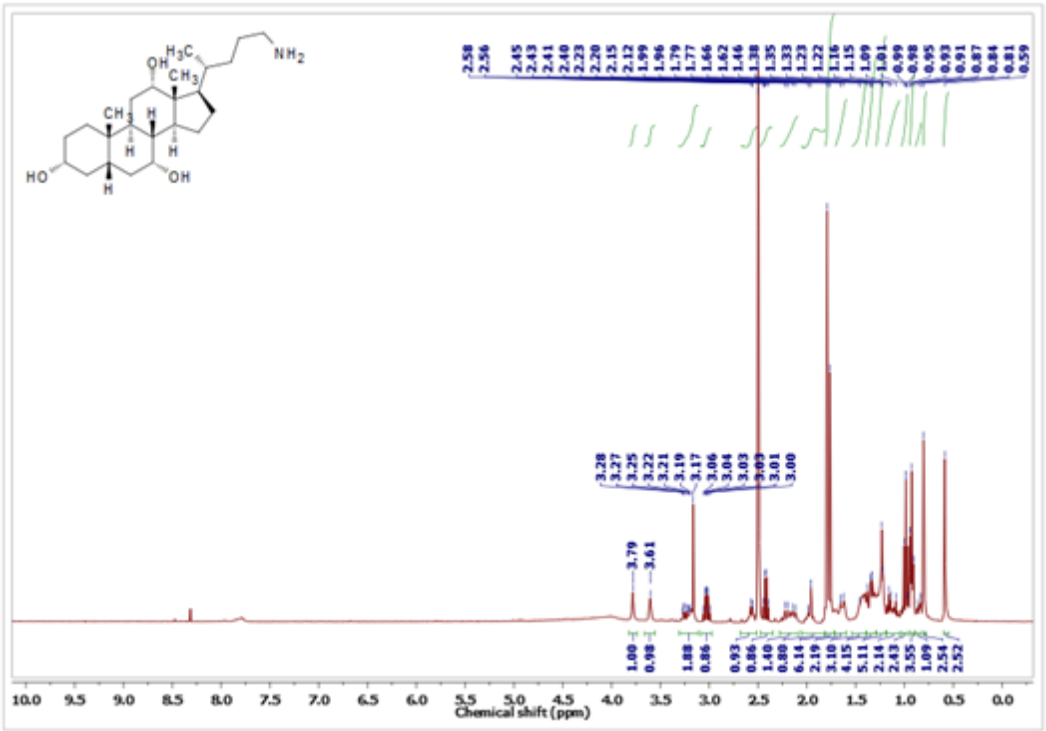

Fig. S17 400 MHz ^{1}H NMR spectrum of **3** in DMSO-d_6.

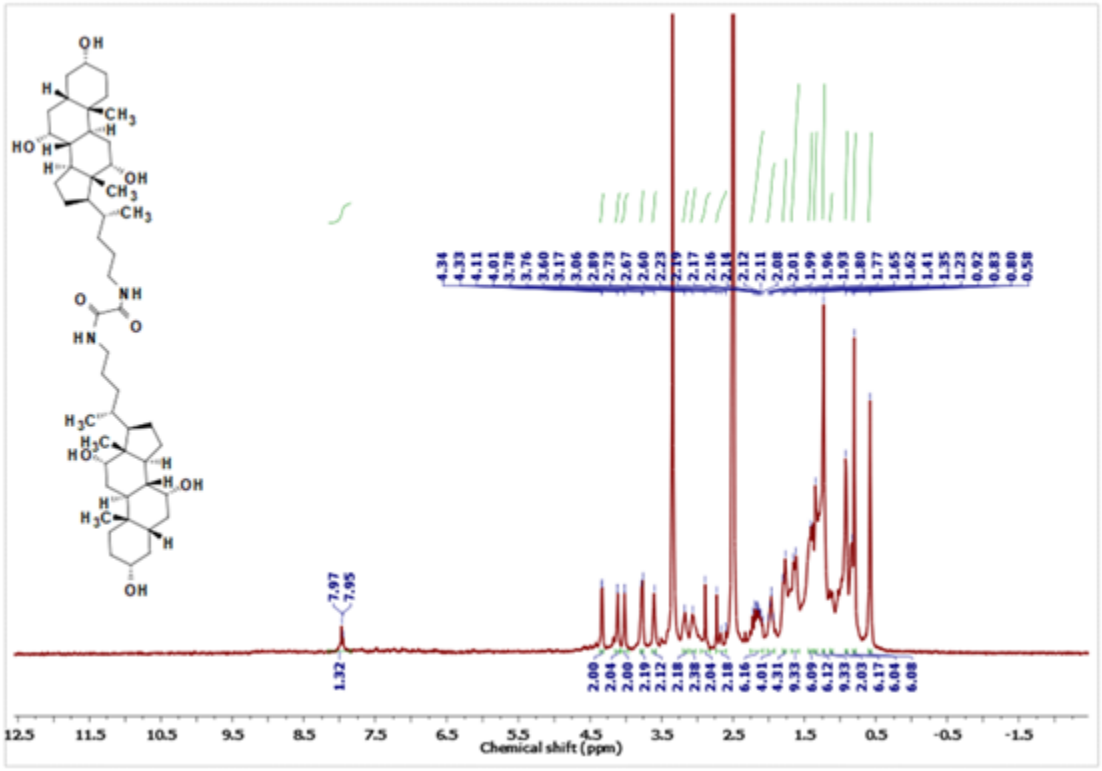

Fig. S18 400 MHz ^{1}H NMR spectrum of **1a** in DMSO-d_6.

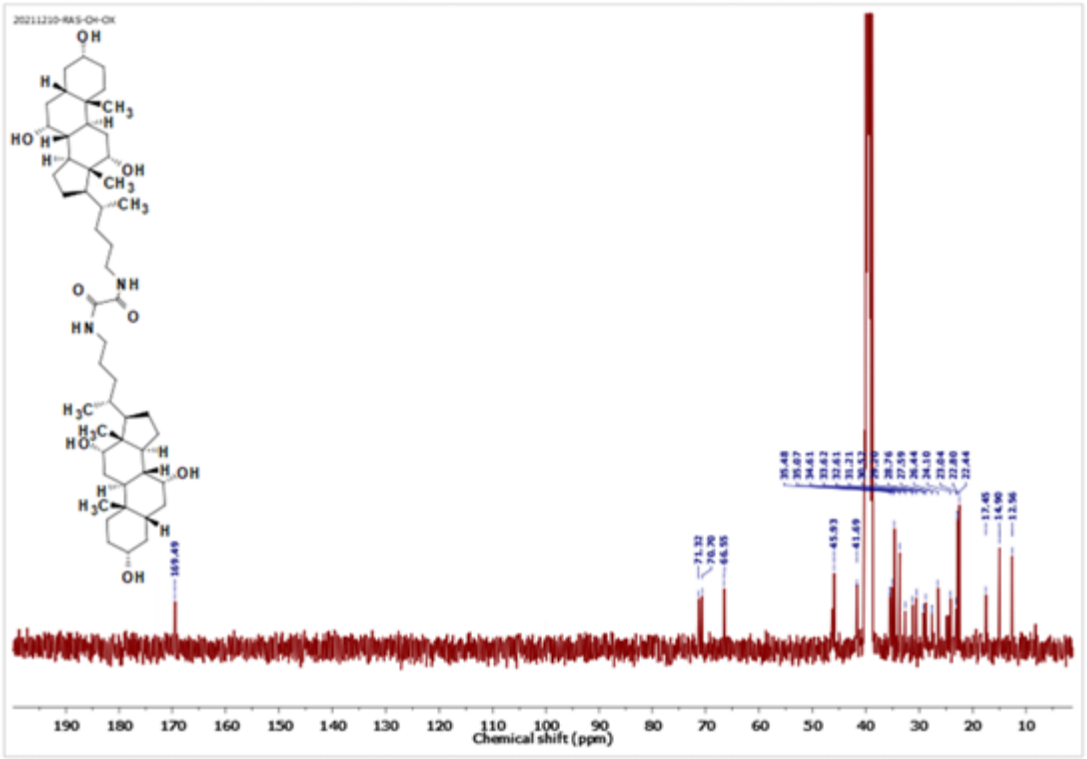

Fig. S19 101 MHz ^{13}C NMR spectrum of **1a** in DMSO-d_6.

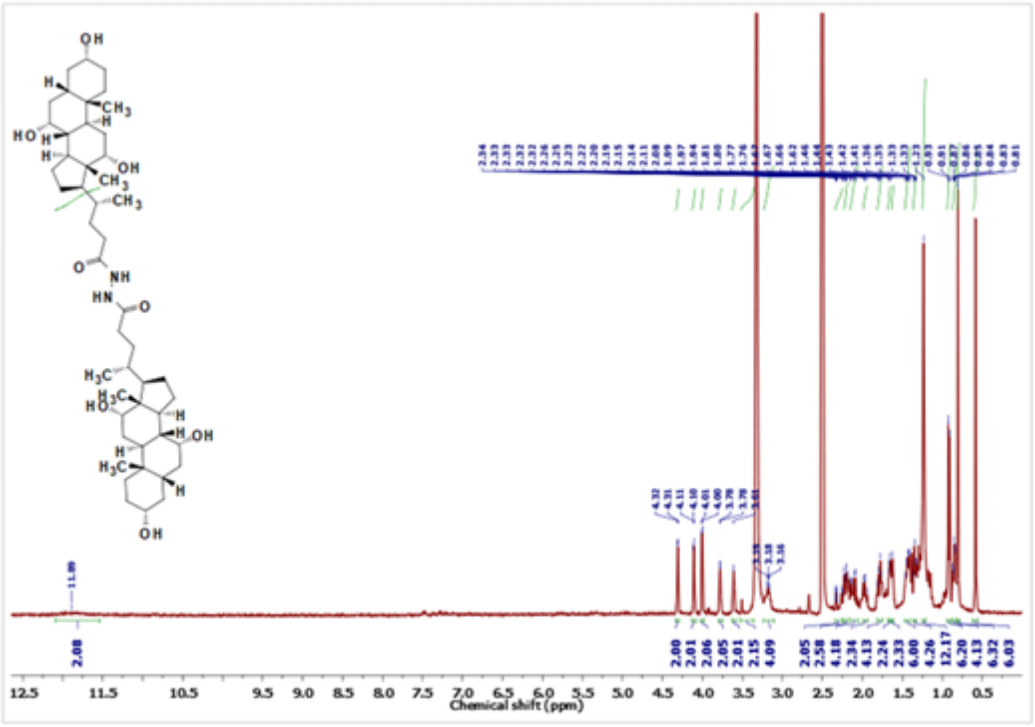

Fig. S20 400 MHz ^{1}H NMR spectrum of **1b** in DMSO-d_6.

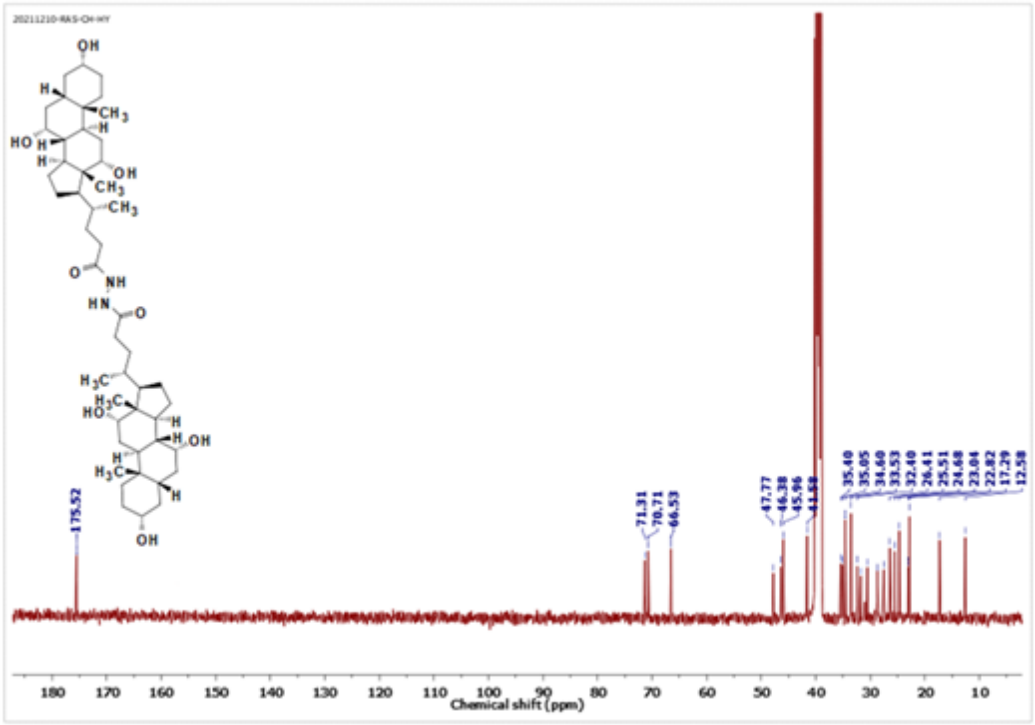

Fig. S21 101 MHz ^{13}C NMR spectrum of **1b** in DMSO-d_6.

VIII. References:

S1 Y. Zhou, E.-H. Ryu, Y. Zhao and L. K. Woo, *Organometallics*, 2007, **26**, 358–364.

S2 a) T. Saha, S. Dasari, D. Tewari, A. Prathap, K. M. Sureshan, A. K. Bera, A. Mukherjee and P. Talukdar, *J. Am. Chem. Soc.*, 2014, **136**, 14128–14135; b) P. Talukdar, G. Bollot, J. Mareda, N. Sakai and S. Matile, *J. Am. Chem. Soc.*, 2005, **127**, 6528–6529; c) V. Gorteau, G. Bollot, J. Mareda, A. Perez-Velasco and S. Matile, *J. Am. Chem. Soc.*, 2006, **128**, 14788–14789.

S3 A. Vargas Jentzsch, D. Emery, J. Mareda, P. Metrangolo, G. Resnati and S. Matile, *Angew. Chem., Int. Ed.*, 2011, **50**, 11675–11678.

S4 S. Bhosale and S. Matile, *Chirality*, 2006, **18**, 849–856.

S5 A. Roy, D. Saha, A. Mukherjee and P. Talukdar, *Org. Lett.*, 2016, **18**, 5864–5867.

S6 N. Sordé and S. Matile, *J. Supramol. Chem.*, 2002, **2**, 191–199.

S7 P. Talukdar, N. Sakai, N. Sordé, D. Gerard, V. M. F. Cardona and S. Matile, *Bioorg. Med. Chem.*, 2004, **12**, 1325–1336.

S8 C. Ren, X. Ding, A. Roy, J. Shen, S. Zhou, F. Chen, S. F. Yau Li, H. Ren, Y. Y. Yang and H. Zeng, *Chem. Sci.*, 2018, **9**, 4044–4051.

S9 J. Domański, P. J. Stansfeld, M. S. P. Sansom and O. Beckstein, *J. Membr. Biol.*, 2010, **236**, 255–258.

S10 T. H. Schmidt and C. Kandt, *J. Chem. Inf. Model*, 2012, **52**, 2657–2669.

S11 H. J. C. Berendsen, J. P. M. Postma, W. F. van Gunsteren and J. Hermans, (1981) Interaction models for water in relation to protein hydration. In: B. Pullman, Ed., Intermolecular Forces, D. Reidel Publishing Company, Dordrecht, 331–342.

S12 C. Oostenbrink, A. Villa, A. E. Mark and W. F. van Gunsteren, *J. Comput. Chem.*, 2004, **25**, 1656−1676.

S13 A. K. Malde, L. Zuo, M. Breeze, M. Stroet, D. Poger, P. C. Nair, C. Oostenbrink and A. E. Mark, *J. Chem. Theory Comput.*, 2011, **7**, 4026–4037.

S14 B. Hess, C. Kutzner, D. van der Spoel and E. Lindahl *J. Chem. Theory Comput.*, 2008, **4**, 435–447.

S15 S. Nose, *Mol. Phys.*, 1984, **52**, 255−268.

S16 M. Parrinello and A. Rahman, *J. Appl. Phys.*, 1981, **52**, 7182−7190.

S17 T. Darden, D. York and L. Pedersen, *J. Chem. Phys.*, 1993, **98**, 10089−10092.